Available online at www.ijournalse.org

Emerging Science Journal

(ISSN: 2610-9182)

Vol. 10, No. 2, April, 2026

Unified Numerical FFR with Adaptive Bandwidth for 5G and Beyond Multilayer Multisector Networks

Muhammad Yaser [1, 2*], Iskandar [1*], M. Sigit Arifianto [1], Khoirul Anwar [3]

[1] *School of Electrical Engineering and Informatics Institut Teknologi Bandung, Jl. Ganesha No. 10, Bandung, Indonesia.*

[2] *Department of Electrical Engineering, Universitas Pancasila, Jakarta, Indonesia.*

[3] *The University Center of Excellence for Advanced Intelligent Communication (AICOMS), Telkom University, Bandung, Indonesia.*

Abstract

The present research introduces a unified numerical formulation for Fractional Frequency Reuse (FFR) and a user composition-based adaptive bandwidth allocation strategy for multi-layer/multi-sector cell architectures. The proposed FFR metric explicitly accumulates sub-band usage across the inner–outer and inter-sector layers, thereby normalizing diverse reuse patterns into a single, consistent number. This formulation remains consistent with the classical definition (reducing to 1/N reuse under certain conditions), approaches full reuse when multi-layer/sector coordination is applied, and provides a simple yet powerful link between reuse configurations and capacity predictions in 5G and beyond networks. Comprehensive simulations based on a realistic urban macrocell environment show that increasing the architectural complexity from a single-layer to a 2-layer 6-sector network results in a remarkable 184% increase in average cell capacity. Furthermore, in the dynamic bandwidth allocation, the inner user-dominated scenario achieves the highest cell capacity, which is 41% higher than that in static bandwidth allocation. At the same time, dynamic allocation also improves fairness in the outer user-dominated scenario, increasing the Jain fairness index by up to 0.444. These results confirm that the combination of the new FFR formulation and adaptive resource allocation significantly improves spectrum efficiency, cell capacity, and fairness, and provides practical guidance for optimizing the implementation of 5G and beyond cellular network deployments.

Keywords:
Multi-Layer Multi-Sector Network;
FFR Factor;
Adaptive Bandwidth Allocation;
User Distribution;
5G.

Article History:

Received:	05	August	2025
Revised:	25	February	2026
Accepted:	04	March	2026
Published:	01	April	2026

1- Introduction

Radio resource allocation is among the crucial issues in fifth-generation (5G) and beyond cellular networks, where rapid growth in mobile data and the number of devices requires highly efficient and flexible spectrum control [1]. Orthogonal Frequency Division Multiple Access (OFDMA) is the dominant scheme among the multiple access technologies in 4G and 5G networks, enabling flexible frequency allocation and supporting various services. However, the spectrum itself is a fundamentally limited resource, and effective utilization of it is essential if 5G's lofty ambitions, like ultra-low latency, extreme connectivity, and massive capacity, are to be achieved [2]. Its move towards heterogeneous networks (HetNets) brings radio resource management with new complexities. Although densification of the network through deployment of small cells can increase spectrum efficiency, it leads to increased inter-cell interference (ICI), specifically for the cell-edge users (CEUs), who experience a poorer signal-to-interference-plus-noise ratio (SINR) and are exposed to co-channel interference (CCI) more [3]. It has been shown in several studies that the most critical network performance issue can shift from spectrum efficiency to handling interference and user service equity [4]. Hence, adaptive and reliable resource allocation mechanisms become even more critical.

* **CONTACT**: 33220312@std.stei.itb.ac.id; iskandar@itb.ac.id

DOI: https://doi.org/10.28991/ESJ-2026-010-02-09

Fractional Frequency Reuse (FFR) is a successful method for balancing spectrum efficiency and interference control in OFDMA-based cellular networks [5]. In FFR, the cellular coverage is usually divided into separate areas, e.g., cell center and cell edge, with different frequency reuse strategies. The cell center often employs a reuse-1 strategy to achieve maximum spectral efficiency. In contrast, the cell edge uses a higher reuse factor, e.g., reuse-3, to mitigate inter-cell interference and improve the quality of service for edge users. To meet the need for higher capacity and more reliable coverage, cellular network planning has evolved from the traditional single-layer cell concept to multilayer and multisector configurations. In a multilayer cell structure, the coverage area is split into concentric inner and outer layers, which allows resource allocation mechanisms to be location-adapted based on user location and changing propagation conditions. In this way, bandwidth, power, and interference can be managed independently for users close to the base station and users at the cell edge, thus improving spectrum efficiency and overall user experience. Additional performance improvement is brought about by sectorization, where each cell is further divided into several angular sectors, most frequently three or six, each served by a directional antenna. When combined with sectorization, multilayer architecture gives rise to the multilayer multisector cell network, in which separate frequency sub-band and power allocation for each sector and layer become possible. This layered and sectorized strategy offers excellent flexibility for optimizing spectral efficiency, interference control, and service quality in modern cellular networks.

Earlier research on Fractional Frequency Reuse (FFR) has typically been concerned with analyzing spectrum efficiency and interference mitigation in a traditional single-layer cellular network. Earlier work, like Nasr-Esfahani & Ghahfarokhi [6] and Alzubaidi et al. [7], investigated the application of FFR for edge user protection and co-channel interference suppression. However, they typically adopted a static or cluster-based frequency reuse factor strategy, usually denoted as 1/N, without taking into consideration the flexibility of subband allocation between various regions of the cell. Dong et al. [8] reaffirmed that while FFR can boost edge user capacity and stifle interference, most of the models applied still presume a static allocation pattern between clusters and fail to provide for the dynamics of inter-layer traffic within the cell. Several subsequent research works, like those by [9-11] developed the FFR concept in heterogeneous networks (HetNets) through analysis of fixed bandwidth sharing strategies and their effects on user capacity and fairness. However, most analytical and planning frameworks still measure reuse factors discretely between clusters, originally formulated for single-layer cells. Classical formulations like these do not explicitly capture intra-cluster reuse arising from inner/outer separation or sectorization. Meanwhile, several other research works [12-15] have considered dynamic bandwidth allocation strategies in dense small cell and ultra-dense networks. However, their emphasis has been more towards cross-cell adaptation mechanisms and load balancing, without incorporating specific bandwidth adaptation between layers and sectors of an individual multi-layer/sector cell.

Several recent studies also point to the contribution of multi-layer networks and sectorization in enhancing spectrum efficiency and capacity. Research by Khan et al. [16], Yin et al. [17] and Xie et al. [18] addresses enhanced inter-cell interference coordination strategies in LTE and 5G HetNet networks and shows that the use of different sectors and layers can enhance frequency reuse and network capacity. However, the treatment of reuse factors in the literature is still discrete and topology-specific, resulting in the lack of a unified numerical metric that simultaneously captures inter-cluster and intra-cluster reuse across layers and sectors. Consequently, there is no architecture-independent analytical bridge from reuse metrics to capacity that applies uniformly from single-layer to 2-layer 3/6-sector.

In several extensive surveys and reviews [19-21] the necessity of combining adaptive resource management and more dynamic frequency reuse schemes is stressed, both in 5G and B5G (Beyond 5G) networks, particularly in high traffic density and user distribution dynamics environments. Integration efforts are also beginning to be aimed at joint optimization among bandwidth allocation, user association, and power control mechanisms [22-24]. Nonetheless, most of these investigations continue to employ a partial approach either solely on the inter-cluster reuse aspect, the layer or sector aspect only, or only on the bandwidth allocation aspect and have yet to show a numerical FFR factor approach that integrally brings together inter-cluster and intra-cluster frequency reuse, as well as flexible adaptation of subband allocation to diverse network topologies and traffic dynamics. This gap forms the foundation for the urgency and primary contribution of this study.

Based on these conditions, there are at least three main gaps in the literature, i.e.,: The absence of a unified numerical FFR factor that simultaneously captures inter-cluster and intra-cluster reuse (due to inner/outer and sectorization), making it difficult to measure effective subband usage per cell in modern multi-layer/multi-sector topologies; There is no rigorous analytical bridge from reuse metrics to capacity applicable across architectures, such as single-layer, 2-layer omni, or 2-layer 3/6-sector, so planners still rely on per-scenario simulations; Comprehensive evaluation of the interaction between bandwidth allocation strategy (static vs. dynamic, user composition-aware) and unified reuse metrics under realistic channel conditions is still limited. Table 1 maps the position of this research among previous FFR works.

This study introduces a unified numerical formulation of the FFR factor, describing the combined reuse of frequency resources in both the inner and outer layers by all cells within a cluster. This definition formulates the FFR factor as the sum of the inner and outer sub-band allocations for all cells, normalized by the number of sub-bands and cells. This can be extended to general multi-layer and multi-sector deployments and offers a more systematic foundation for spectrum

efficiency analysis, channel capacity assessment, and resource allocation optimization in future cellular networks. In addition, an adaptive and context-aware resource allocation scheme is introduced, whereby bandwidth is allocated dynamically between the inner and outer layers in response to real user distribution, traffic patterns, and real-time channel conditions. This allows responsive adjustment of spectrum allocation to changes in the number of users per layer or sector, optimizing cell capacity and enhancing fairness among users. By taking propagation, interference, and mobility characteristics into account, this scheme is adaptable to a range of urban and ultra-dense environments. It accommodates a variety of service demands in 5G networks and beyond. This research contributes to addressing these gaps by:

- Formulates a unified numerical FFR factor that sums the utilization of inner and outer layer subbands (and sectors if any) per cell, then normalized over the number of subbands and cells. This formulation generalizes the classical reuse (1, 1/3, 1/6) as a limit case, and allows intermediate values up to near full-reuse in coordinated multi-layer/multi-sector operations;
- Linking these factors to capacity through a unified capacity formulation at the cell and cluster level, so that the numerical FFR factor becomes a direct predictor of capacity for a variety of topologies (ranging from single-layer, 2-layer omni, to 2-layer 3/6-sector);
- Integrates an adaptive bandwidth allocation strategy based on inner/outer user proportion, maintaining resource constancy and monotonicity with respect to load (relevant for strategy comparison on two-layer FFR);
- Conducts a comprehensive simulation study (3GPP UMa/NR) modeling inter/intra-cell interference, explores three user compositions (75/25, 50/50, 25/75 inner/outer) and two allocation strategy (static vs. dynamic), and reports cell & per-user capacity, CDF, and Jain's fairness metrics. Results show a pattern of capacity increase with increasing architectural complexity, starting from single-layer, then 2-layer omni, then 2-layer 3-sector, up to 2-layer 6-sector, and identify conditions where dynamic allocation is superior to static allocation.

Table 1. Comparison of related study

Study Group	Topology & Reuse Focus	Bandwidth Allocation Treatment	Contribution / Gap Addressed
Classic FFR [5, 7, 11, 16, 25]	Typically, multi-layer; FFR reduces co-channel interference for edge users.	Static, discrete 1/N reuse.	Lacks a unified numeric reuse metric across topologies.
FFR in HetNets [4, 6, 9, 23]	Heterogeneous networks; reduce inter cell interference	Static (fixed sharing).	Still uses discrete inter-cluster reuse; does not model adaptive inter-layer strategy.
Present research	Multi-layer (inner/outer) & multi-sector (3/6); three user mix scenarios (75/25, 50/50, 25/75). Evaluate capacity, fairness	Static vs Dynamic (proportional to users per layer).	Closes the gap, provides a unified numeric FFR factor (inter & intra-cluster) directly tied to capacity across architectures.

The results of this research provide important insights into how adaptive and contextual resource allocation mechanisms, combined with the proposed FFR factor formulation, can improve capacity, spectrum efficiency, and fairness in next-generation mobile networks. These findings not only enhance academic understanding but also provide practical guidance for operators to optimize 5G and beyond system deployments amidst changing traffic dynamics and user distribution.

The rest of this paper is structured as follows. Section 2 describes the system model and explains the network and user scenarios examined in this work. Section 3 explains the unified numerical formulation of the FFR factor and gives a user distribution configuration of multi-sector and multi-layer networks. Section 4 provides a complete analysis of cell capacity with various fractional frequency reuse schemes. Section 5 explains the simulation parameters and settings, provides the simulation results, and discusses the effect of user distribution and bandwidth allocation schemes on the performance of multi-sector and multi-layer cells. Section 6 concludes the paper.

2- System Model

The network models investigated in this research are composed of multilayer cells and multilayer cells with sectors. In the case of multilayer cells, as indicated in Figure 1(b), the cell coverage area is partitioned into two layers, i.e., the inner layer and the outer layer, where each user is labeled as an inner or outer user based on their location with respect to the cell center. Meanwhile, in the multilayer cell multi-sector model, each cell is also partitioned into inner and outer layers, but with various sector configurations. Figures 1(c) and 1(d) respectively sketch the use of the sectorization principle in multilayer cells, where the cell coverage area is partitioned into several sectors based on the network design requirements.

In multi-layer and multi-sector architectures, each sector is modeled with a directional antenna with a specific facing direction. The beamwidth is narrowed in 3-sector or 6-sector configurations so that the transmitted energy is more focused forward and the sidelobes/backlobes are more damped. Power is normalized per base station, so that the power delivered to each sector scales inversely with the number of sectors, the total base-station power remains constant. Interference consists of two components: intra-site (between sectors within a base station), which is reduced by inter-

sector isolation, and inter-site (between neighboring sectors), which is calculated only when the antenna orientation is within the relevant angle threshold (angle filter). This definition makes interference calculations more realistic and efficient for multi-sector scenarios.

In each structure, the available bandwidth in the system is organized into two portions: one portion is assigned to the inner layer and shared by all users in the cell center region, and the other portion is assigned to the outer layer and further divided into several segments, each of which is assigned to sectors in the outer layer. Through this mechanism, bandwidth usage becomes more adaptive and can be tuned to the user distribution characteristics and traffic demand in each sector, optimally handling spectrum efficiency and possible interference between users.

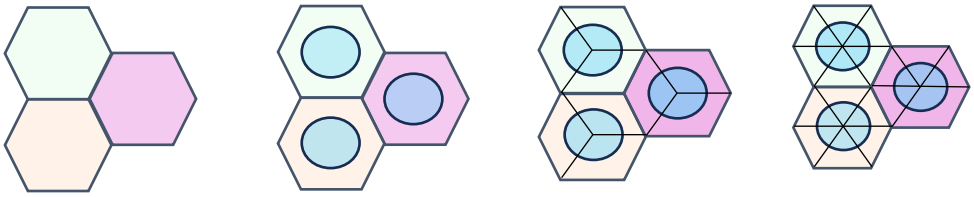

Figure 1. Layerization and sectorization for 5G networks

In order to gain a complete view of the effects of architectural complexity, user distribution, and bandwidth allocation strategies on network performance, simulation scenarios were designed systematically. The users were randomly distributed within the cell's coverage area in each simulation run, with different proportions of inner and outer users to reflect various traffic conditions. Figure 2 shows three user distribution scenarios: 75 inner and 25 outer users, 50 inner and 50 outer users, and 25 inner and 75 outer users. For every scenario, two bandwidth allocation strategies were evaluated: static allocation, in which the bandwidth allocation for the inner and outer layers is fixed irrespective of the number of users, and dynamic allocation, in which the bandwidth allocation is changed proportionally according to the number of users in each layer at any instance. In the dynamic bandwidth allocation test, the configuration used was 2-layer without sectors (omni).

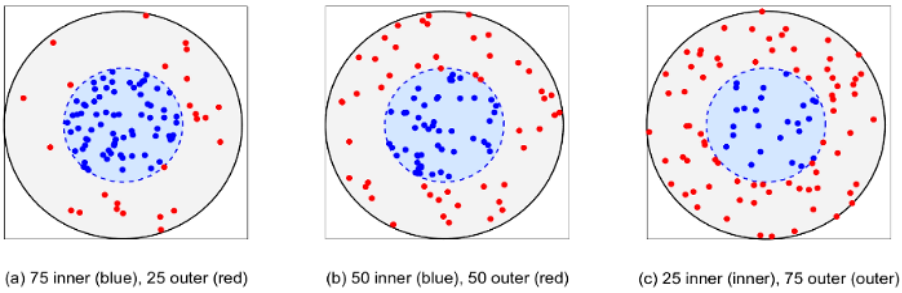

Figure 2. Distribution of inner and outer users in a two-layer cell for three user allocation scenarios

The channel environment for this simulation was modeled based on a typical urban macrocell, considering the impact of path loss and interference between layers and sectors. All users are assumed to be active and fully use the resources assigned to them. The whole simulation procedure is executed using a Monte Carlo method over many iterations to make the results possess high statistical meaning and reflect the impact of random user location and distribution variations on overall network performance. Under this simulation platform, the impact of multilayer implementation, sectorization, user distribution, and adaptive bandwidth management on spectrum efficiency, service distribution fairness, and user experience quality can be fully assessed. The results emphasize the significance of resource allocation strategy and network architecture design in maximizing capacity and fairness in cellular systems.

3- Unified Numerical FFR Factor and Adaptive Bandwidth Allocation for User Distribution

This section provides the methodology and a detailed analytical framework for Fractional Frequency Reuse (FFR) in multi-layer cellular networks, accounting for theoretical formulations and applications in realistic network configurations. Figure 3 summarizes the methodology, starting with system modeling (single-layer, 2-layer omni, and 2-layer 3/6-sector) and the definition of a unified numerical FFR that generalizes inter-/intra-cluster reuse, followed by the correlation between capacity and the channel & interference model (3GPP UMa). Next, user composition scenarios (75/25, 50/50, and 25/75) are combined with static and adaptive bandwidth allocation strategies. The final stage is Monte Carlo simulation, metric calculation (cell-per-user capacity, CDF, and Jain's fairness), and comparative analysis across architectures and strategy. The exposition is divided into two primary subsections. First, we propose a unified numerical

formulation for the FFR factor, allowing for more accurate quantification of frequency resource reuse in evolved network topologies. The formulation extends traditional frequency reuse concepts and serves as a basis for investigating networks with layered and sectorized structures. Second, we outline the user distribution model and bandwidth allocation strategy employed in simulations to assess network performance under different traffic conditions. By systematically varying the ratio of inner and outer users and adopting static and dynamic bandwidth allocation strategies, the present study seeks to capture the impact of user heterogeneity and adaptive resource management on primary performance metrics. The formal definition of the FFR factor is outlined in Sub-section 3.1, while Sub-section 3.2 outlines the bandwidth allocation mechanisms employed in this work.

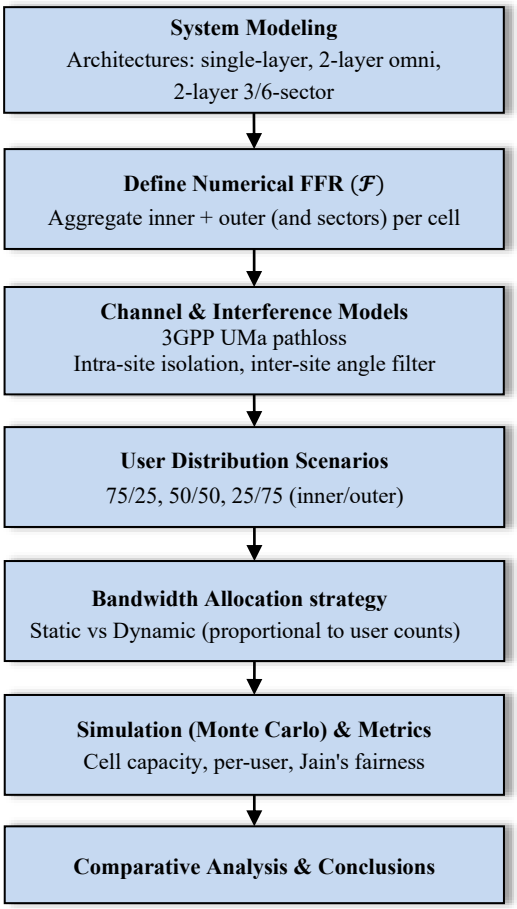

Figure 3. Methodology flowchart of Numerical FFR-based evaluation for multi-layer/sector cellular networks

3-1- The Proposed Numerical Formulation of FFR Factor

The effective utilization of frequency resources is one of the major principles for designing modern cellular networks, particularly with multi-layer and sectorized deployments in 5G networks. The frequency reuse (FR) factor has been used to represent the ratio of spectrum being reused between cells or clusters. This typically only considers inter-cluster reuse and disregards possible reuse within clusters since traditional networks have no layer separation. In modern multi-layer and multi-sector cells, the definition of Fractional Frequency Reuse (FFR) is more involved since frequency subbands can be assigned separately to various layers (e.g., inner and outer) or sectors within the same cell. This added flexibility allows for more dynamic and efficient spectrum allocation, but it also complicates the process of quantifying frequency reuse and its impact on network performance. As such, the traditional approach to calculating the FR factor is no longer sufficient for capturing the complexities of resource allocation in advanced network architectures. Hence, to generate a more accurate and generalized metric, this work introduces a unified numerical formulation for the FFR factor that can be applied to intra-cluster and inter-cluster reuse in arbitrary network setups. Unlike the conventional definition of frequency reuse, which captures only inter-cluster reuse (1/N), our proposed numerical FFR factor explicitly aggregates subband usage within clusters (inner/outer and sector), thereby generalizing both inter-cluster and intra-cluster reuse. The factor acts as an effective multiplier on the total system capacity. In a single-layer reuse-N scenario, returns to 1/N as per the classical definition. When the network is organized into two layers and multiple sectors with more even and coordinated subband usage, it can approach 1, indicating near maximum spectrum utilization. This new formulation provides a unified framework for analyzing frequency resource utilization across different network topologies, enabling researchers and network planners to better assess and optimize the spectral efficiency of multi-layer and multi-sector deployments.

Suppose a cellular system has a total bandwidth divided into D orthogonal subbands. These subbands can be flexibly allocated to the inner and outer areas of each cell, with varying reuse patterns. Assume there are N cells in a cluster. For each i_{-th} cell (i=1, 2..., N_i), f_{in} and f_{out} represent the number of subbands allocated to the inner and outer layers, respectively. The proposed numerical formulation of the FFR factor is as follows:

$$\mathcal{F} = \sum_{i=1}^{N} \frac{(f_{in}+f_{out})_i}{N \cdot D} \quad (1)$$

$$= \frac{1}{N \cdot D} \sum_{i=1}^{N} (f_{in} + f_{out})_i \quad (2)$$

where, N is a number of cells in a cluster, D is a total number of subband, f_{in} is a part of subbands allocated for inner layer of a cell, and f_{out} is part of subbands allocated for outer layer of a cell.

This formulation represents the average fraction of frequency resources that are effectively reused across all layers and cells within a cellular network cluster. This means that the FFR factor $\mathcal{F}$ indicates the proportion of the total subbands allocated to both the inner and outer layers relative to all available subbands within the cluster. The benefit of this definition is that it can provide flexible and tailored subband allocation patterns for every cell in the inner and outer layers. This is especially applicable in multi-layer and multi-sector networks, where resource allocation strategy may differ among cells due to traffic requirements, number of users, and local channel characteristics. Thus, this metric not only calculates conventional frequency reuse (e.g., inter-cluster reuse) but also depicts the dynamics of composite and adaptive subband usage in modern network environments (see Table 2).

Table 2. Comparison of Conventional FR/FFR and the Proposed Numerical FFR Factor

Aspect	Conventional FR/FFR	Numerical FFR (Proposed)
Scope	Primarily inter-cluster (reuse across cells/clusters)	Inter- and intra-cluster simultaneously (accumulates inner/outer and sectors if present)
Metric	Discrete reuse ratio: $\mathcal{F} = \frac{1}{N}$ (e.g., 1/3, 1/6)	Numerical factor: $\mathcal{F} = \frac{1}{ND}\sum_{i=1}^{N}(f_{\text{in},i} + f_{\text{out},i})$
Architecture	Single-layer, does not capture layering/sectorization	Multi-layer / multi-sector ready, captures per-layer/sector subband allocation
Operational meaning	Indicates spectrum share per cell only across clusters	Indicates effective subband share used across all cells & layers (normalized average)
Limits	Fixed at $\frac{1}{N}$	Covers $\frac{1}{N}$ (classical case), can approach 1 (full reuse with coordination), and yields intermediate values (partial multilayer/sector)
Analytical usefulness	Suits simple architectures	General basis for capacity/SE analysis and planning in modern 5G/B5G multi-layer/sector networks

Furthermore, this formulation allows for a more comprehensive and realistic analysis of spectrum efficiency and frequency resource reuse. This provides a solid foundation for assessing capacity performance, interference management, and optimal frequency planning schemes in future cellular network rollouts, especially in the case of multi-layer, multi-sector cell, and non-homogeneous user distribution scenarios. This proposed definition of the FFR factor generalizes the conventional concept of frequency reuse, which is limited to inter-cluster reuse. In single-layer cellular systems, intra-cluster reuse is not possible due to the lack of spatial separation; however, with the advent of a multi-layer architecture, frequency resources can be allocated and reused more flexibly, both within and between clusters. Therefore, the FFR factor is highly relevant for analyzing channel capacity, spectrum utilization, and interference management in modern and future cellular networks.

3-2- User Distribution and Bandwidth Allocation Strategies

To fully assess the effect of user distribution and bandwidth allocation schemes on the performance of multi-layer cellular networks, this work systematically analyzes several typical traffic scenarios. Specifically, three user proportion scenarios are considered to capture different traffic density patterns frequently observed in real network deployments: (a) 75 users in the inner layer and 25 users in the outer layer, (b) 50 inner users and 50 outer users, and (c) 25 inner users and 75 outer users. In each simulation run, the users are randomly placed within the cell coverage area and labeled as inner or outer users according to their distance from the cell center compared to a predefined threshold radius (the inner layer radius). This method is aimed at capturing the dynamics of user location as seen in real life, where traffic density can be concentrated close to the base station or stretched to the cell edge, based on the time of day, environment, or specific service requirements.

Along with these variations in user distribution, two different bandwidth allocation schemes are implemented to assess their effectiveness in managing spectrum resources and maintaining service quality. Static bandwidth allocation divides the total available bandwidth into fixed portions for each layer (inner and outer), regardless of the actual number

of users in each layer. This strategy is easy to implement, but it can potentially result in inefficient spectrum utilization, especially when user distribution is highly imbalanced, as bandwidth at one layer can become underutilized while another layer becomes overloaded.

In contrast, dynamic bandwidth allocation aims to improve resource utilization efficiency and service equity by adjusting the bandwidth allocated to each layer proportionally to the actual number of users in that layer at any given time. In this scheme, if a layer has more users, a larger proportion of the allocated bandwidth will be allocated, resulting in a more responsive and balanced spectrum resource distribution. This approach is particularly advantageous in environments with fluctuating user density or highly uneven distribution, as it can minimize resource waste and optimize overall network capacity. The dynamic bandwidth allocation evaluation in this paper is performed on a 2-layer sectorless (omni) architecture to isolate the effect of allocation strategy from the benefits of sectorization.

We define a two-layer (inner–outer) spectrum allocation strategy that is proportional to the user load. At each evaluation interval t, the bandwidth allocation fractions for the inner and outer layers are determined by the ratio of the number of active users in each layer to the total system users. Formally, with $\mathrm{U_i(t)}$ and $\mathrm{U_o(t)}$ denoting the number of users in the inner and outer layers, respectively, and $\mathrm{U(t) = U_i(t) + U_o(t)}$ and $\mathrm{B_{tot}}$ denoting the total system bandwidth, the allocation fraction is given by

$$\alpha_i(t) = \frac{U_i(t)}{U(t)} \tag{3}$$

$$\alpha_o(t) = 1 - \alpha_i(t) \tag{4}$$

Consequently, the amount of bandwidth allocated to each layer is

$$B_i(t) = \alpha_i(t)\, B_{tot} \tag{5}$$

$$B_o(t) = \alpha_o(t)\, B_{tot} \tag{6}$$

This formulation preserves resource conservation $(\mathrm{B_i(t) + B_o(t) = B_{tot}})$ and is monotonic with respect to load allocation fraction increases as $\mathrm{U_i(t)}$ relative to U(t) increases, making it suitable for analyzing allocation strategy comparisons on two-layer FFR architectures in a scalable and replicable manner. Through a combined study of user distribution and bandwidth allocation strategies, this study aims to develop a deep understanding of their impacts on key performance metrics, such as total cell capacity, capacity per user, fairness index, and cumulative user capacity distribution.

4- Analysis on The Capacity of Fractional Frequency Reuse

This section presents a comprehensive analysis of channel capacity in cellular networks implementing Fractional Frequency Reuse (FFR), with particular emphasis on how the numerical FFR factor $\mathcal{F}$, which is determined by the number of layers and sectors in the network architecture, fundamentally affects the achievable network capacity

4-1- Capacity Formulation

At the core of this analysis using of a unified, numerical expression for the frequency reuse factor. For the i_{th} cell, the channel capacity is defined by the extended Shannon formula [25]:

$$C_i = \mathcal{F} \cdot B \cdot \log_2(1 + \gamma_i) \tag{7}$$

where B is the total system bandwidth, γ_i being the SINR of a user at the i_{th} cell. $\mathcal{F}$ is the frequency reuse factor reflecting the fraction of bandwidth actively utilized in the network. The total capacity for a cluster of N cells is thus:

$$C_t = \sum_{i=1}^{N} C_i = \mathcal{F} \sum_{i=1}^{N} B \cdot \log_2(1 + \gamma_i) \tag{8}$$

This formulation clearly establishes that the FFR factor is directly proportional to the cluster's total capacity, making it a key determinant in the design and optimization of cellular networks.

4-2- Pathloss Model for 5G cellular Network

A realistic estimation of cellular network capacity critically depends on the adoption of an appropriate pathloss model, particularly in 5G scenarios with heterogeneous deployment environments and a wide range of operating frequencies. In this study, the 3GPP Urban Macro (UMa) pathloss model for 5G New Radio (NR) is used to model signal propagation between the base station (BS) and user equipment (UE) over inner and outer cell areas.

The pathloss (PL) in decibels (dB) is formulated as:

$$PL = 28.0 + 40 \log_{10}(d_{3D}) + 20 \log_{10}(f_c) \; - 9\, log_{10}((d'_{BP})^2 + (h_{BS} - h_{UT})^2) \tag{9}$$

The pathloss model considers several essential parameters: d_{3D}, the direct distance between the base station antenna height h_{BS} and the user terminal height h_{UT}, both in meters; f_c, the carrier frequency in Hertz; and d'_{BP}, the breakpoint

distance marking the change in propagation characteristics. These parameters collectively enable accurate modeling of signal attenuation for various deployment scenarios in 5G networks.

By using the 3GPP 5G pathloss model, the simulation accurately reflects the propagation conditions found in modern 5G networks so that the resulting capacity and frequency reuse analysis is relevant to practical deployment scenarios. This approach provides a robust foundation for evaluating the impact of architectural enhancements such as additional layers and sectors on spectral efficiency under realistic channel conditions. In addition, the use of a standardized pathloss model ensures comparability with other studies and facilitates benchmarking of different network configurations. Such consistency is essential for drawing generalizable conclusions and supporting evidence-based network planning decisions.

4-3- Single Layer Cluster

In the single-layer scenario shown in Figure 1(a), there is no inner/outer separation, so the inner-layer contribution is zero $(\mathrm{f}_{\mathrm{in,i}} = 0)$. The total bandwidth is divided into D subbands that are grouped into three mutually exclusive pools between cells (reuse-3). Since the reuse-3 strategy gives each cell only one of the three pools, for each cell i $\mathrm{f}_{\mathrm{out,i}} = \frac{\mathrm{D}}{3}$ holds. Substitution into Equation 2, Numerical FFR with $\mathrm{N} = 3$ yields;

$$\mathcal{F}_s = \frac{1}{3D}\sum_{i=1}^{3}\left(0 + \frac{D}{3}\right) = \frac{1}{3} \tag{10}$$

This narrative shows that the proposed numerical formulation reduces exactly to the classical reuse $\mathcal{F}_s = 1/3$ when single layer with exclusive band partitioning between cells. Based on Equation 7 each cell's capacity becomes;

$$C_1 = C_2 = C_3 = \frac{1}{3}B\log_2(1+\gamma) \tag{11}$$

And the total cluster capacity is:

$$C_t = C_1 + C_2 + C_3 = B\log_2(1+\gamma) \tag{12}$$

This shows that the lower the FFR factor (with fewer layers and sectors), the more limited spectrum utilization and network capacity are, because most of the spectrum is not used in each cell to minimize interference between cells.

4-4- Multi-Layer Cluster

Moving to the two-tier architecture shown in Figure 1(b), the B band is divided into four subbands $(\mathrm{f}_1, \mathrm{f}_2, \mathrm{f}_3, \mathrm{f}_4)$. One subband, $\mathrm{f}_4 = \frac{1}{4}\mathrm{B}$, is dedicated to the inner layer and is shared (reuse-1) by all cells to serve UEs near the BS with low interference, so that for each cell i $\mathrm{f}_{\mathrm{in,i}} = 1$ (in units of "number of subbands"). The other three subbands $(\mathrm{f}_1, \mathrm{f}_2, \mathrm{f}_3)$ are shared for the outer layer and are reuse-3-arranged between cells in a three-cell cluster, so that each cell uses only one distinct outer subband and gives $\mathrm{f}_{\mathrm{out,i}} = 1$. Thus, each cell effectively utilizes two of the four subbands, i.e., $\mathrm{f}_{\mathrm{in,i}} + \mathrm{f}_{\mathrm{out,i}} = 2$. Plugging this into the Equation 2 for $\mathrm{N} = 3$ and $\mathrm{D} = 4$ becomes,

$$\mathcal{F}_m = \frac{1}{3\cdot 4}\sum_{i=1}^{3} 2 = \frac{1}{2} \tag{13}$$

So that the numerical FFR factor increases from 1/3 in the single-layer reuse-3 to 1/2 in the two-layer configuration, reflecting richer spectrum utilization without sacrificing interference control. The channel capacity for the i-th cell is

$$C_i = (C_{in} + C_{out})_i, \tag{14}$$

where, C_{in} is the capacity for inner layer, and C_{out} as the capacity of outer layer.

The capacity for each cell, as the sum of inner and outer layer contributions, is:

$$C_i = \frac{1}{4}B\log_2(1+\gamma_{in}) + \frac{1}{4}B\log_2(1+\gamma_{out}) \tag{15}$$

$$= \frac{1}{2}B\log_2(1+\bar{\gamma}) \tag{16}$$

Aggregating across three cells, the total capacity is:

$$C_t = C_1 + C_2 + C_3 \tag{17}$$

$$= 3\left(\frac{1}{2}B\log_2(1+\bar{\gamma})\right) \tag{18}$$

$$= \frac{3}{2}B\log_2(1+\bar{\gamma}) \tag{19}$$

where, $\bar{\gamma}$ is the average SINR for inner and outer layers.

By increasing the number of layers, the numerical FFR factor increases, which directly increases effective bandwidth utilization and achievable network capacity. This layered structure allows for more flexible and efficient frequency planning without significantly increasing interference.

4-5- Multi Layer Multi Sector Cluster

In a two-layer, three-sector cell as shown in Figure 1(c), the B band is still divided into four subbands (f_1, f_2, f_3, f_4). Subband $f_4 = \frac{1}{4}B$ is used as an inner layer with reuse-1 to serve users near the BS in all three sectors of each cell. The other three subbands (f_1, f_2, f_3) are allocated to the outer layer and split per sector within each cell, for example, sector A uses f_1 , sector B uses f_2, and sector C uses f_3 . At the same time, inter-cell coordination maintains a reuse-3 pattern to keep co-channel interference at the sector/cell boundaries low. With this scheme, the set of unique subbands actually used by a cell is a complete four subbands, i.e., one inner subband and three outer subbands. Since the total subbands $D = 4$ and the number of cells per cluster N = 3, based on Equation 2 numerical FFR becomes

$$\mathcal{F}_{ms} = \frac{1}{3 \cdot 4}\sum_{i=1}^{3}(1+3) = 1 \tag{20}$$

This shows that sectorization allows effective utilization of the entire band per cell, with the inner shared and the outer orthogonalized within sectors within the cell and coordinated between cells. In practice, the measured value can be slightly below one due to guard/control and SINR limitations. Still, conceptually the numerical FFR for 2-layer three sectors leads to $F \approx 1$, higher than both the 2-layer unsectored ($\mathcal{F}_m = 1/2$) and the single-layer reuse-3 ($\mathcal{F}_s = 1/3$) cases. The channel capacity for the i-th cell is:

$$C_i = (C_{in} + C_{out})_i \tag{21}$$

where, C_{in} is the capacity for inner layer, and C_{out} as the capacity of outer layer

The capacity for each cell, summed over its sectors, is:

$$C_i = \frac{1}{4}B\log_2(1+\gamma_{in}) + \frac{3}{4}B\log_2(1+\gamma_{out}) \tag{22}$$

$$= B\log_2(1+\overline{\gamma}) \tag{23}$$

Thus, the total cluster capacity becomes:

$$C_t = 3(B\log_2(1+\overline{\gamma})) \tag{24}$$

where, $\bar{\gamma}$ denotes the mean SINR across all sectors and layers.

From the above analysis, it is clear that the numerical FFR factor plays a key role in capacity enhancement in modern cellular networks. As network architectures evolve from simple single-layer designs to more complex multi-layer and multi-sector topologies, the FFR factor value increases gradually from $\mathcal{F}_s = \frac{1}{3}$ for single-layer (low capacity), $\mathcal{F}_m = \frac{1}{2}$ for multi-layer (medium capacity), to $\mathcal{F}_{ms} = 1$ for multi-layer multi-sector (maximum capacity). With the proposed numerical form of the FFR factor applied, network planners can analytically predict and maximize the gains in spectral efficiency achievable with additional layers and sectors. This integrated analytical framework enables a systematic network evolution process, enabling capacity targets to be efficiently achieved through intelligent architectural development and frequency planning.

5- Simulation Results and Discussion

The primary aims of this simulation are to suggest and verify a comprehensive and unified numerical formulation of the FFR factor that best captures frequency resource reuse in intricate multi-layer and multi-sector network topologies; to examine systematically the effect of user distribution and bandwidth allocation strategies (static vs. dynamic) on major performance metrics such as aggregate cell capacity, per-user capacity, and the Jain Fairness Index and to examine the effect of static vs. dynamic bandwidth allocation on the performance of the network. And to quantify the gains of multi-layer and sectorized structures over conventional single-layer cell configuration. Furthermore, this work examines the effectiveness of dynamic resource allocation in improving spectrum usage, capacity, and fairness among users Performance evaluation employs holistic metrics such as aggregate cell capacity, per-user capacity, fairness index, and cumulative distribution function (CDF) analysis, giving a synoptic view of how architectural complexity, user heterogeneity, and adaptive resource management strategies can be judiciously combined to enhance spectrum efficiency and quality of service in future cellular networks.

In this study, simulation uses a realistic urban macrocell network model. Key parameters such as bandwidth (100 MHz), carrier frequency (3.5 GHz), cell radius, base station transmit power, and noise density are configured according to the 3GPP TR 38.901 specification. We use a 3.5 GHz carrier with 100 MHz bandwidth, the mid-band configuration

commonly used in 3GPP UMa macro scenarios, enabling realistic capacity range trade-offs for multilayer/multisector planning. While the channel model used here follows 3GPP UMa, the proposed numerical FFR factor applies across frequency bands and acts as an effective multiplier on capacity; thus, the framework remains applicable to both sub-6 and mmWave bands by substituting the appropriate channel / SINR model. This study uses a snapshot-based Monte Carlo method. At each iteration, user positions are reshuffled to generate multiple independent snapshots of the network state, while the number of inner and outer users remains constant. We do not model user movement or changes over time. Therefore, the reported capacity and fairness metrics reflect performance variability across spatial snapshots rather than changes over time. This choice was made intentionally to ensure the influence of architecture (multilayer/multisector) and allocation strategy (static vs. dynamic) is clearly and cleanly visible, without temporal interference. We calculate thermal noise using the standard kTB formula. The SINR at each snapshot is then converted to data rate using the Shannon limit, so that performance comparisons remain consistent and independent of specific models. Transmit power is normalized per-site across all topologies, for sectored cells the total site power is divided evenly across the active sectors to ensure fair comparisons and allow capacity gains to be attributed to the architecture, not to additional power. Interference calculations include both intra-site and inter-site components: leakage between sectors within a site is suppressed by the assumption of sector isolation. In contrast, inter-site interference is governed by the reuse pattern and antenna directivity toward users.

Different network scenarios are systematically investigated to explore the impact of user distribution, bandwidth allocation strategies, and network architecture on system performance. The architectures studied include single-layer cells, multi-layer cells with separate inner and outer regions, and multi-layer, multi-sector cells where each cell is further divided into three or six sectors, each with its inner and outer regions. To demonstrate the diversity of traffic patterns, three scenarios of user distributions are examined: 75 inner users and 25 outer users, a balanced case of 50 inner users and 50 outer users, and 25 inner users and 75 outer users. Users are randomly distributed within the coverage and divided according to their distance from the cell center. Two bandwidth allocation methods are compared: static, in which a fixed bandwidth fraction is allocated to each layer, and dynamic, in which the bandwidth is split adaptively according to the number of users in each layer.

All ‘dynamic bandwidth’ results in this section refer to a 2-layer, unsector (omni) cell configuration. The compared static results use the same 2-layer omni baseline to isolate sectorization effects. Users are randomized at each iteration and labeled inner/outer based on a threshold radius (Rth). Results are summarized with aggregate and per-user capacities, CDF, and Jain's fairness index. In the 2-layer unsectored (omni) architecture, the inner layer operates with reuse-1, while the outer layer reuses spectrum with neighboring cells, leading to inter-cell interference. The details of the simulation parameters can be seen in Table 3. This parameter selection is in line with the common 3GPP UMa mid-band implementation, and can be transferred to other frequencies by changing the corresponding path-loss and SINR models without changing the numerical FFR framework.

Table 3. Simulation Parameter

Parameters	Values
Cell radius	5000(m)
Inner layer radius	2500(m)
Transmit Power of inner layer	50 dBm
Transmit Power of outer layer	53 dBm
System Bandwidth	100MHz
Frequency	3.5 GHz
Number of users	100
Boltzmann constant	1.38×10^{-23}
Temperature	300K

Simulation results are shown and discussed to demonstrate the effect of different network architectures, user distribution scenarios, and bandwidth allocation schemes on overall network performance. The discussion concentrates on a number of important performance measures, including total cell capacity, capacity per user, fairness index, and CDF distribution. Every graph emphasizes a particular feature of system performance, with close comparisons across the considered scenarios. In the following, a close interpretation of these simulation results is presented, with a close explanation of every graph in order to determine the merits and trade-offs of every configuration.

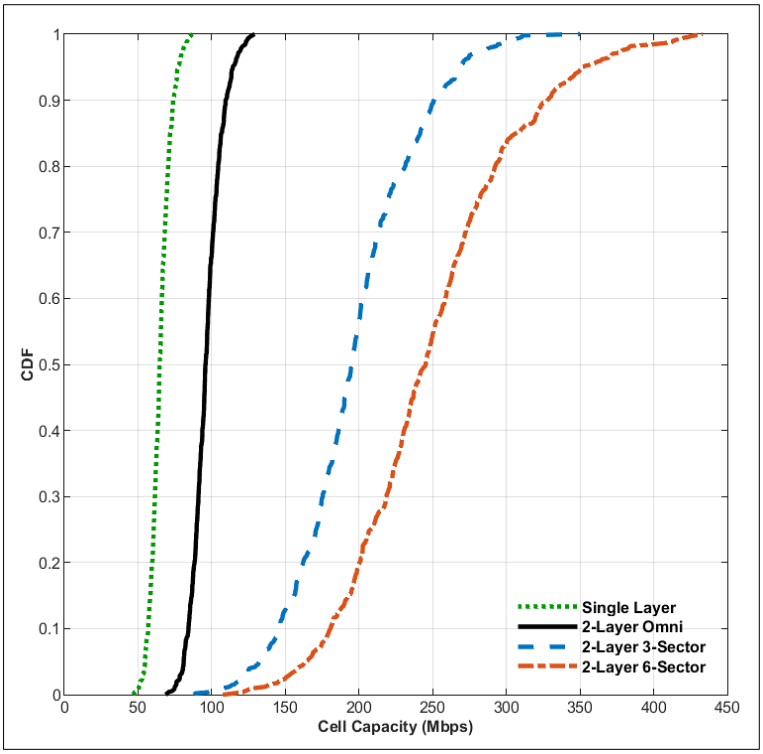

Figure 4. Comparison of the cell capacity between single layer cells and multilayer multisector cells

Figures 4 and 5 collectively provide a comprehensive evaluation of cell capacity performance across various network architecture scenarios, including single-layer, 2-layer omni, 2-layer 3-sector, and 2-layer 6-sector designs. Figure 4 shows the Cumulative Distribution Function (CDF) curves for cell capacity across four network architecture scenarios. The steeper slopes of the single-layer and 2-layer omni curves indicate lower inter-run variability but also lower capacity ceilings. In contrast, the wider sector curves reflect higher rate levels across the distribution. The simulation results clearly show that the distribution of cell capacity in the single-layer scenario tends to be on the left, indicating lower capacity values than in the multilayer and sectorized scenarios. This position on the left side is consistent with more substantial channel interference and the absence of inter-sector isolation in an omnidirectional configuration. Conversely, the CDF curve for the 2-layer 6-sector scenario is farthest to the right, indicating a significant and consistent increase in capacity across all simulation iterations. This behavior stems from the main-lobe narrowing and per-sector orthogonalization, which "thin out" the dominant interferer and increases the SINR for a larger portion of users. In the single-layer scenario, the majority of cell capacity lies in the 50–100 Mbps range, with a 90% probability that the capacity does not exceed 100 Mbps. In other words, the 100 Mbps target will be achieved in only about 1 in 10 realizations in this environment.

Meanwhile, implementing the 2-layer omni architecture shifts the CDF curve to the right, with a 90% probability that the capacity does not exceed approximately 150 Mbps. An even greater increase is observed in the sectorized scenario. In both the 2-layer 3-sector and 2-layer 6-sector scenarios, the CDF curves widen to the right as capacity increases, with 90% probability that the capacities do not exceed approximately 250 Mbps and 350 Mbps, respectively. At the 200 Mbps service target, the likelihood of meeting the rate is not small in the 3-sector case and is much higher in the 6-sector case, highlighting the reliability benefits of sectorization. This confirms that dividing cells into sectors reduces interference and increases spectrum utilization efficiency. This achievement aligns with the proposed numerical FFR factors: sectorization and inner/outer separation increase the effective subband fraction per cell, thereby implying higher capacity through the unified capacity link. In general, this CDF graph shows that the more complex the network architecture, with multilayer and sectorization implementations, the higher the probability that a cell achieves high capacity. This CDF also provides a quantitative overview of the quality of service guarantees that can be completed in each scenario. The minimum guaranteed capacity for a large number of users increases significantly in the multi-sector scenario compared to the single-layer scenario. This increase comes from improvements in SINR (interferer attenuation) and increased effective subband reuse within the cell.

Figure 5 supports these findings by graphing the average cell capacity for all architectures. The graph shows an increase in capacity with increasing network architecture complexity. The single-layer scenario could only support an average capacity of 65.04 Mbps. This low mean is consistent with a left-shifted CDF and reflects the strong interference binding of omnidirectional reuse. Enhancing the architecture to a 2-layer omni model increased the average capacity to 96.32 Mbps, about 48% higher than the single-layer case. This increase is due to separating inner and outer resources

so that the inner layers can exploit higher reuse without burdening edge users. The implementation of sectorization had a far greater effect; the average capacity in the 2-layer, 3-sector case amounted to 197.08 Mbps, and even rose to 248.90 Mbps in the 2-layer, 6-sector case. The jump from omni to 3-sector roughly doubles the average capacity (~+105%), while the increase from 3 to 6 sectors adds another ~26% showing a decreasing but still significant yield. The results are unmistakable: cell sectorization is a highly effective method for boosting network capacity, reducing user interference within each sector, and improving bandwidth utilization efficiency. It is important to note that all scenarios are evaluated with the same per-site power normalization and channel environment, so the observed improvements come solely from the topology and reuse patterns, not from additional power or bandwidth. Also, a multi-layer architecture has been found to maximize frequency resource utilization by separating users based on their distance from the base station, enabling more adaptive power and bandwidth allocation as needed. This layering also opens up strategy flexibility (e.g., static vs adaptive bandwidth) that can be tuned to traffic composition, as analyzed in the following sections.

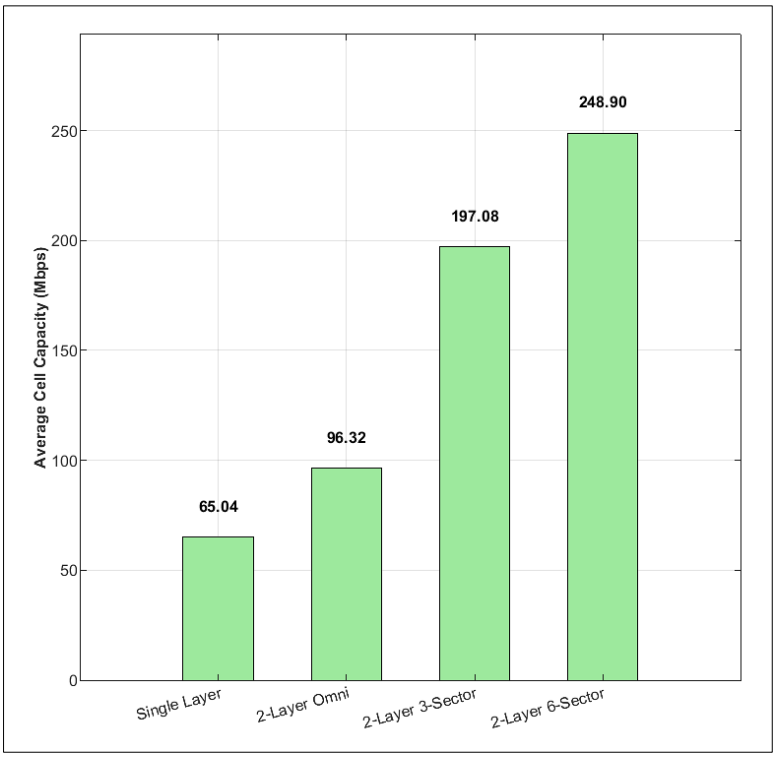

Figure 5. Average cell capacity comparison of single-layer and multi-layer sectorized networks

The CDF curves of cell capacity under static bandwidth allocation for three different user configuration scenarios in a multilayer cellular network are presented in Figure 6. Since the bandwidth distribution between the inner and outer layers is fixed under a static strategy, the total capacity depends heavily on how users are distributed across the two layers. Each curve illustrates the probability that the total cell capacity does not exceed a given value under the specified user distribution. In reading the CDF, a shift of the curve to the right at the same percentile indicates greater confidence in achieving the target rate. In contrast, a steeper slope indicates less inter-simulation variability. The simulation results demonstrate that the scenario with a higher proportion of inner users (75 inner, 25 outer) achieves the rightmost CDF curve, indicating consistently higher cell capacity than the other scenarios. This order approximates first-order stochastic dominance: the 75:25 curve is to the right of 50:50, and 50:50 is to the right of 25:75 at most percentiles. On the other hand, the outer-dominating setting (25 inner, 75 outer) produces the left-shifted CDF curve, showing decreased overall cell capacity. With static allocation, the outer layer becomes a bottleneck when many users are at the cell edge because its portion of the spectrum cannot be expanded to follow load spikes.

This is the trend in which increasing the number of inner users closer to the BS, with lower path loss and lower interference, significantly enhances overall cell capacity. Mechanistically, inner users have stronger signals and fewer dominant interferers, resulting in higher spectral efficiency per Hz, and as the number increases, the total capacity accumulates. On the other hand, a larger number of outer users reduces performance, as they experience weaker signal reception and more severe intercell interference. In addition, fixed sharing can underutilize the inner layer when the number of inner users is small, resulting in some high-efficiency subbands being wasted and a decrease in total capacity. From a quality-of-service perspective, this result offers a visual and quantitative measure of achievable capacity guarantees for each scenario. For example, at CDF 0.9, the total cell capacities are ≈ 23,600 Mbps for 75:25, ≈ 16,600

Mbps for 50:50, and ≈ 9,500 Mbps for 25:75. The inner-dominant scenario's guaranteed cell capacity is much greater than that of the outer - dominant scenario. Practically, this implies that static allocation is suitable when the user composition is relatively stable; in environments with a volatile inner/outer ratio, an adaptive bandwidth strategy is more appropriate to avoid under-provisioning when edge users dominate the load. This emphasizes that a user distribution biased towards the inner layer is more favorable for overall network capacity. In contrast, a majority of outer users experience lower network performance due to greater interference and path loss. Thus, Figure 6 not only ranks scenarios by achievable capacity but also guides strategy selection: if the network frequently experiences heavy traffic on the outer edge, static partitioning should be reconsidered in favor of adaptive rules or stronger cell-edge coordination.

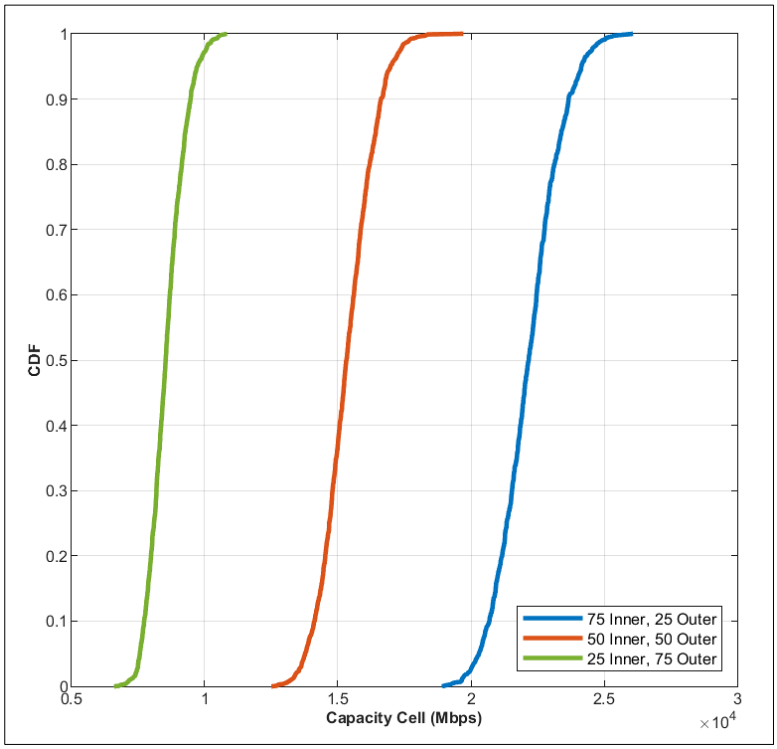

Figure 6. Multi-layer cell capacity under static bandwidth allocation for various user distributions

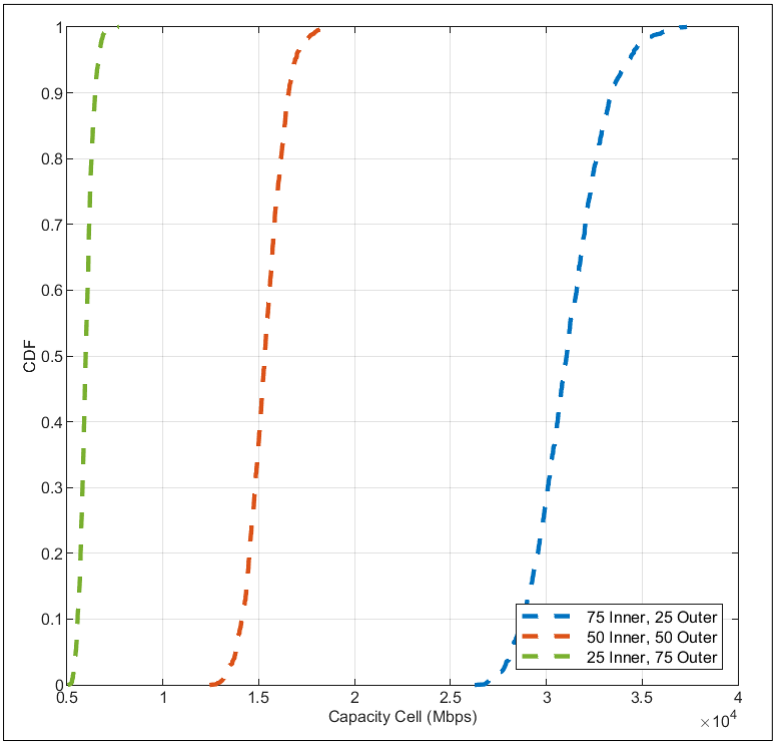

Figure 7. Multi-layer cell capacity under dynamic bandwidth allocation for various user distributions

The cumulative distribution function (CDF) of total cell capacity for three user distribution scenarios in a multilayer cellular network employing dynamic bandwidth allocation is illustrated in Figure 7. In adaptive strategy, the bandwidth allocation between inner and outer layers is adjusted based on user composition, so that the total capacity is highly influenced by user location, which dictates the spectral efficiency per Hz. The results clearly show that the scenario with the highest proportion of inner users (75 inner, 25 outer) consistently achieves the highest cell capacity, as indicated by the rightmost CDF curve (CDF 0.9 ≈ 33,500 Mbps). This shows greater reliability in meeting a given rate target across percentiles, as the majority of users operate under better SINR conditions. Conversely, the case dominated by outer users (25 inner, 75 outer) has the worst cell capacity, as indicated by the leftmost CDF curve (CDF 0.9 ≈ 6,500 Mbps). Even though adaptive strategy channel more spectrum to the outer layer, spectral efficiency remains low due to path loss and cell-edge interference, so the additional bandwidth is not fully converted into increased capacity. The middle case (50 inner, 50 outer) is between these two extremes, as one would anticipate (CDF 0.9 ≈ 16,500 Mbps). This trend is due to inner users being closer to the base station, experiencing lower path loss and less intercell interference. Mechanistically, inner users have a higher signal-to-interference ratio, so the bits/Hz per unit bandwidth are higher and accumulate into a larger cell capacity.

Therefore, allocating a larger share of bandwidth to inner users dramatically increases the overall cell capacity. This also explains why, in the inner-dominant composition, the adaptive strategy shifts the CDF curve farther to the right than the static strategy: bandwidth is directed to the most spectrally productive layer. On the other hand, a higher proportion of outer users reduces total cell performance due to increased signal attenuation and greater susceptibility to intercell interference. In the outer-dominant scenario, adaptive strategy tend to reduce spectrum congestion without penetrating the low spectral efficiency limit, leaving the performance gap with the inner-dominant scenario wide. Furthermore, the CDF plots demonstrate that dynamic bandwidth allocation can provide more adaptive resource allocation based on user location. Still, the underlying user distribution remains a decisive factor in determining cell capacity. In other words, adaptive strategy are necessary but not sufficient: without improving cell edge conditions (e.g., inter-cell coordination/power enhancement/subband reordering), capacity will remain limited by the quality of the outer channel. For example, at a CDF value of 0.9, the guaranteed cell capacity for 75:25 is much greater than for 25:75, indicating better quality of service for networks with more inner users. Ensuring a higher share of inner users in the cell is shown to be advantageous for maximizing capacity and achieving better quality of service guarantees under dynamic resource allocation.

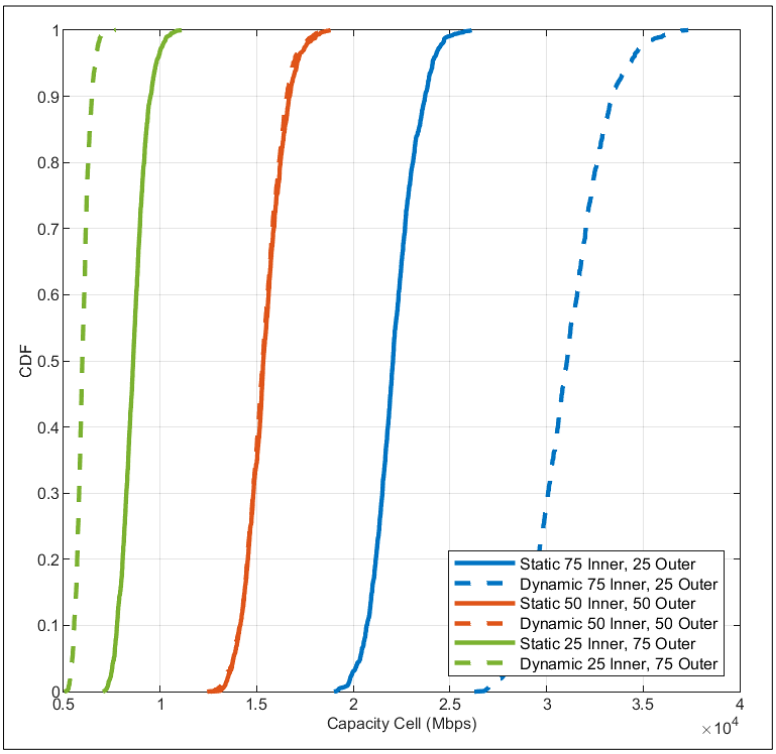

Figure 8. Comparison of multi-layer cell capacity for various user distributions under static and dynamic allocation

Figures 8 and 9 show a comparison of various user distributions under static and dynamic allocation. The CDF plot of capacity in Figure 8, obtained via simulation, reveals a remarkable effect of both the user distribution across the inner and outer layers and the bandwidth allocation strategy used. In other words, performance is not just a function of "how much bandwidth" but also "where the bandwidth is placed" relative to the channel quality of each layer. This confirms

that allocating resources to higher-spectral-efficiency layers (inner) provides systematic capacity gains. In the case of a higher inner-to-outer user ratio (75 inner, 25 outer), the overall cellular capacity is significantly larger with dynamic bandwidth allocation (CDF 0.9 ≈ 33,500 Mbps vs ≈ 23,500 Mbps). This happens because most of the bandwidth is shifted to the inner layer, which has a higher SINR, so each Hz produces more bits (higher spectral efficiency), pushing the CDF curve further to the right. Dynamic bandwidth allocation can adjust resource allocation in proportion to the number of users in each layer. Consequently, bandwidth waste in the layer with fewer users can be reduced, and resource usage in the layer with more users can be maximized. In contrast, in static bandwidth allocation, a fixed amount of bandwidth is reserved for the outer layer regardless of the number of users, resulting in inferior aggregate capacity. In an inner-dominant composition, the fixed allocation leaves some of the high-efficiency subbands in the inner band underutilized.

This fixed reserve in the outer band limits the potential rate because some high-efficiency subbands in the inner band cannot be fully utilized when the inner band is dominant. In scenarios where the number of users is balanced between the inner and outer layers (50:50), both static and dynamic bandwidth allocation effectively distribute resources in similar proportions, whether fixed or adaptive. With static bandwidth allocation, the division is already set proportionally (e.g., 50% for inner users and 50% for outer users), ensuring optimal utilization of network resources based on the actual user distribution. Therefore, adaptive gains are minimal because there are no compositional imbalances to correct. Similarly, dynamic bandwidth allocation, which allocates bandwidth in real time based on user proportions, will also result in a 50-50 split in this case. Therefore, there is no significant advantage of either strategy in terms of aggregate cellular capacity when user distribution is balanced (CDF 0.9 ≈ 16,700 Mbps for both of them). For scenarios with a majority of users in the outer layer (25 inner, 75 outer), the simulation results show that aggregate cellular capacity is actually higher with static bandwidth allocation (CDF 0.9 ≈ 9,500 Mbps vs ≈ 6,500 Mbps). This is because adding a portion of bandwidth to the outer layer (via adaptive) has a small marginal value; the outer layer is at a low SINR, so that additional Hz is not directly proportional to additional bits. This is because static allocation in such cases is already sufficiently proportional to user needs in each layer. Meanwhile, dynamic bandwidth allocation tends to reduce aggregate capacity under these conditions, as a portion of resources is allocated to outer users who, on average, experience poorer channel quality. In other words, adaptive strategy are necessary but not sufficient without improving cell-edge quality.

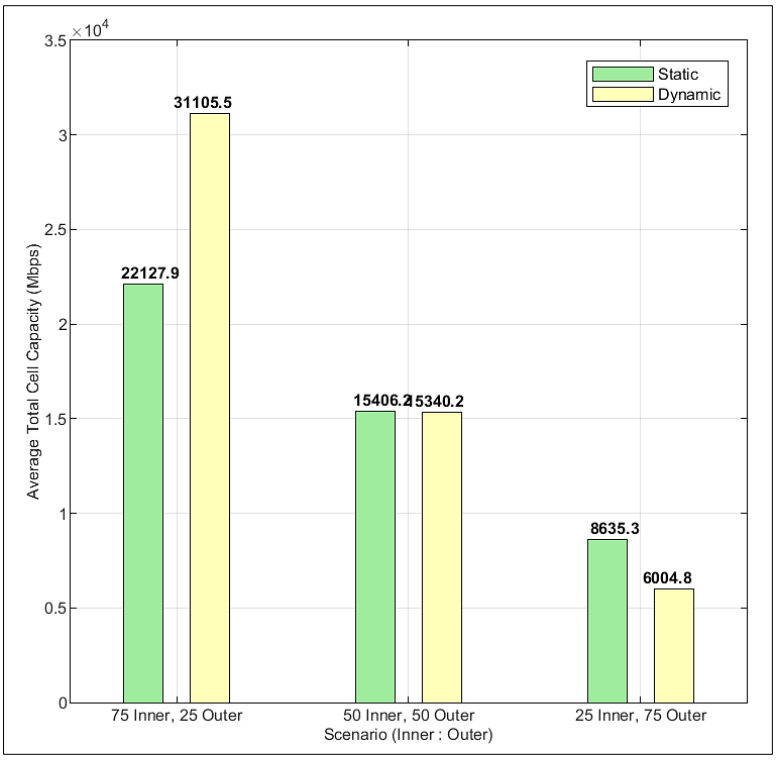

Figure 9. Average multi-layer cell capacity under static and dynamic allocation bandwidth for various user distributions

This trend is substantiated numerically in Figure 9, which plots the average total cell capacity across the three user distribution scenarios, each tested with two bandwidth allocation strategies: static and dynamic. For example, in the 75 inner, 25 outer scenarios, the average cell capacity is 22,127 Mbps for static bandwidth allocation and rises sharply to

31,105 Mbps for dynamic allocation. This 41% increase is consistent with the logic of placing bandwidth in the most spectrally productive layer. Mechanistically, the majority of users are in good SINR conditions (inner), so each additional Hz results in a significant bit gain; adaptive allocation minimizes spectrum "waste" in less dense layers. However, in the 50 inner, 50 outer scenarios, both static and dynamic bandwidth allocations yield nearly identical average capacities: 15,406 Mbps and 15,340 Mbps, respectively. The minimal difference confirms that balanced composition eliminates the need for adaptation. In the 25 inner, 75 outer scenario, the average cell capacity is higher with static bandwidth allocation (8,635 Mbps) than with dynamic allocation (6 Mbps). This shows that allocations that push too much spectrum to low-SINR tiers actually reduce aggregate capacity.

These findings show the significant impact of user spatial distribution on the performance of bandwidth allocation methods. In other words, method performance is determined more by "where the user is" than simply by "how much bandwidth" is shared. Thus, network operators must remain constantly aware of user distribution patterns to select the best allocation scheme dynamically. By implementing a context-aware, adaptive allocation mechanism, the network can respond more effectively to traffic heterogeneity and temporal fluctuations, thereby minimizing the risk of capacity loss during peak or uneven usage periods. Ultimately, such an adaptive strategy enables cellular networks to maintain high, consistent performance and spectral efficiency across a range of operating conditions. In summary, these findings underscore that the bandwidth allocation strategy for multilayer cellular networks must be tailored to the prevailing user distribution. It's important to note that all scenarios are compared at the same per-site power and total bandwidth, so performance differences stem purely from resource allocation between layers, not from additional power/spectrum. Dynamic bandwidth allocation works exceptionally well when there is a significant imbalance in user distribution across layers. In contrast, static allocation is more suitable when user distribution is even or when most users are in the outer layer. As such, an adaptive bandwidth allocation strategy that can adapt to changing user distribution patterns is vital to today's cellular networks to maximize aggregate capacity and achieve efficient network resource utilization.

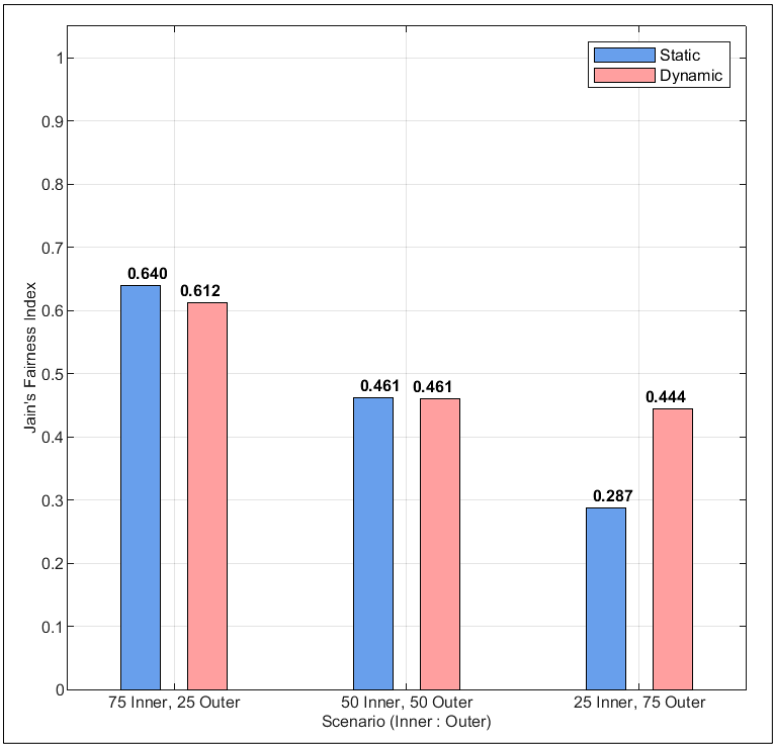

Figure 10. Fairness Index for various user distributions under static and dynamic bandwidth allocation

The bar chart of Jain's Fairness Index plotted in Figure 10 offers more than a numerical comparison. The Jain Index measures fairness (0–1); the closer to 1, the more equitable the capacity distribution among users is, but not necessarily the highest average capacity. First, while the static allocation yields the highest fairness index (0.640) in the 75 inner, 25 outer scenarios, this should be interpreted in the context of both resource surplus and demand localization. In an inner-dominant scenario, fixed allocation tends to be "naturally aligned," with many users' demands residing in layers with good SINR, so that inter-user variation decreases and fairness increases without the need for dynamic adjustments. The inner users, benefiting from closer proximity to the base station and better channel conditions, receive ample resources under both allocation strategies. Consequently, the inner–outer gap

narrows in this scenario, and increased fairness does not significantly compromise aggregate capacity. Static allocation divides bandwidth according to a fixed proportion that, in a scenario dominated by inner users, closely matches user demand, resulting in high fairness.

This finding is consistent with the previous CDF, which showed the curve shifting to the right when the majority of users are located in the inner region. Conversely, in the 25 inner region, 75 outer region scenario, dynamic allocation's higher fairness index (0.444 vs. 0.287 for static) underscores a key advantage: adaptability to channel and user demand heterogeneity. Here, adaptive allocation acts as a compensatory redistribution, allocating more spectrum to the outer region, which is marginalized by path loss and interference, thus narrowing the capacity disparity between users. Outer users, typically experiencing worse signal quality and higher path loss, are often underserved when static allocations persist, especially when the resource allocation does not scale with user distribution. This is why the static fairness index falls low; fixed strategies do not keep pace with the increasing number of users in the outer region. Dynamic allocation mitigates this by reallocating bandwidth in real time based on users' actual locations, thereby narrowing the capacity gap between well-served and poorly-served users. However, it should be noted that an increase in fairness in outer-dominant conditions can be offset by a decrease in aggregate capacity, resulting in a trade-off between efficiency and equity. This improvement in fairness translates directly into a better user experience for those at the cell edge, helping to reduce service complaints, improve coverage, and fulfill regulatory or operator targets for minimum guaranteed service levels. The 50:50 scenario is especially illuminating from a network planning perspective: the identical fairness indices (0.461) for both strategies indicate that, when user distributions match the allocation ratios, the choice between static and dynamic becomes less relevant than fairness.

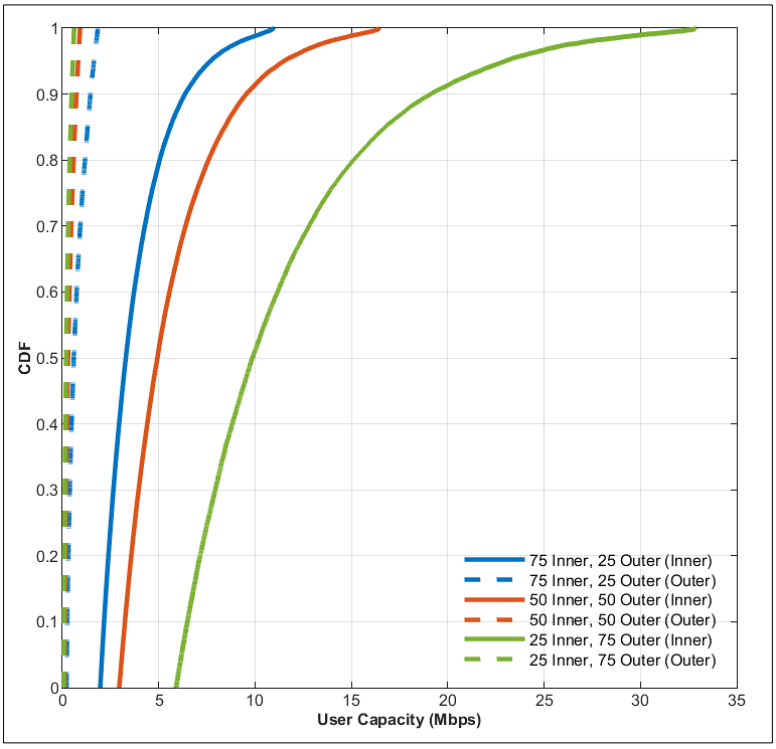

Figure 11. User Capacity under static bandwidth allocation for various user distributions

Figure 11 illustrates the user capacity in simulations with static bandwidth allocation between the inner and outer layers, where each layer receives a fixed portion of bandwidth regardless of the number of users. In a static strategy, the per-user capacity is primarily determined by (i) the channel quality/SINR of each layer and (ii) the per-user bandwidth allotment, which is inversely proportional to the number of users in that layer; therefore, changes in user composition immediately shift the CDF curve. The performance gap in user capacity between layers is highly influenced by user distribution. In the scenario dominated by inner users (75 inner, 25 outer), the bandwidth per inner user is lower because it is shared among more users; however, their capacity remains high thanks to their proximity to the base station and lower interference levels (CDF 0.9 ≈ 6.4 Mbps**)**. This indicates that the SINR gain in the inner layer (greater spectral efficiency/bits per Hz) outweighs the decrease in per-user bandwidth allotment, so the inner CDF curve remains far to the right. Conversely, although outer users in this system receive a larger per-user bandwidth share, their capacity is lower because they are farther from the base station and experience greater interference (CDF 0.9 ≈ 1.5 Mbps). Additional Hz in the outer layer are not fully converted into bits due to path loss and cell-edge interference, so the outer CDF curve accumulates in low-capacity areas. In the balanced scenario (50 inner, 50 outer), the bandwidth per user is

more evenly distributed across both layers, resulting in average capacity values for each group that fall between the two extreme cases (inner CDF 0.9 ≈ 9.6 Mbps; outer CDF 0.9 ≈ 0.8 Mbps).

The steeper slope of the curve in the balanced case indicates minor inter-run variations because the per-user bandwidth allowance and channel quality are at a relatively stable compromise. In the scenario with a majority of outer users (25 inner, 75 outer), inner users enjoy a larger bandwidth per user because of their smaller numbers, maintaining high capacity (CDF 0.9 ≈ 19 Mbps). In contrast, outer users experience a decline in capacity due to the increasingly limited bandwidth per user and consistently high interference. In general, these findings indicate that with static bandwidth allocation, adding more users to a single layer reduces the average capacity in that layer, especially in the outer layer, highlighting the need for careful user distribution and resource allocation strategies to balance fairness and performance demands in network services. The CDF graph in Figure 11 shows that inner users consistently receive higher capacity than outer users, regardless of the distribution scenario. This dominance is consistent with the interference model: users near the base station experience fewer dominant interferers, leading to higher spectral efficiency. The sharp outer curve in low-capacity areas highlights service limitations for users at the cell edge, especially when the number of outer users is dominant. This finding confirms that static bandwidth allocation cannot yet address the performance gap between layers. Thus, static strategy needs to be combined with other strategies (or replaced by adaptive allocation based on user composition) to narrow the inner-outer performance gap without sacrificing aggregate capacity.

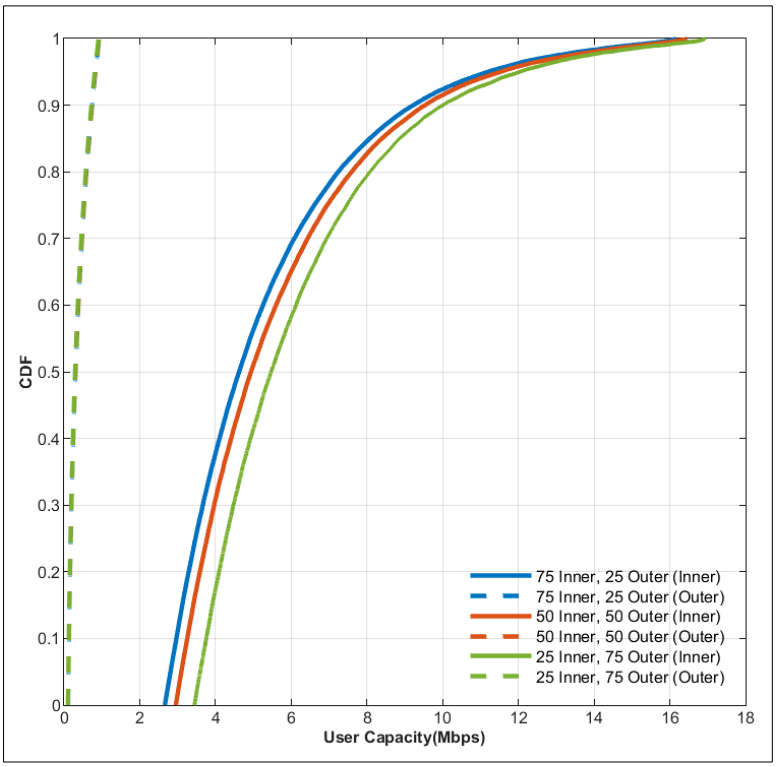

Figure 12. User Capacity under dynamic bandwidth allocation for various user distributions

Figure 12 shows the CDF of the capacity per user comparison across three inner and outer user distribution scenarios with dynamic bandwidth allocation. In the adaptive strategy, bandwidth is divided proportionally according to the number of users in each layer, so the resulting capacity is primarily determined by the user's location (inner/outer), which controls the spectral efficiency per Hz. In each scenario, bandwidth is divided proportionally based on the number of users in each layer. The simulation results show that the CDF curves for inner users are always to the right of those for outer users across all scenarios, indicating that most inner users achieve higher capacity than outer users. This is consistent with the SINR advantage of inner users (closer to the base station and facing fewer dominant interferers), resulting in higher bits/Hz per unit bandwidth at almost all percentiles. In the 75 inner:25 outer scenario, the capacity of inner users is relatively lower because the allocated bandwidth must be shared among many users. In contrast, outer users have the smallest capacity among all scenarios due to their small number, so the portion of dynamic bandwidth allocated to them is tiny. The implication is that, in this scenario, the inner-outer gap is primarily driven by "spectrum limitations" on the outer side; the outer layer's bandwidth is small and unable to compensate for channel weaknesses at the cell edge. Conversely, in the 25 inner users:75 outer users' scenario, inner users enjoy the highest capacity because of their smaller number. Still, the majority of outer users must share bandwidth with many other users, so the capacity per outer user remains low, though slightly better than in the 75:25 scenario.

The outer users' dominance reduces the bandwidth per outer user while keeping the SINR low, causing the outer CDF curve to shift firmly to the left even though the adaptive strategy has increased the spectrum allocation for the outer layer. Meanwhile, the 50:50 scenario provides relatively balanced performance between the two layers, as seen from the curves that lie between the two extreme scenarios. In a balanced composition, adaptive tends to produce a closer 50-50 tuning, resulting in tighter performance for both layers and reduced variability between simulations. The capacity gap between inner users across these three scenarios is not too large, as evidenced by the proximity of the inner CDF curves. Despite changes in the number of users, dynamic bandwidth allocation maintains the performance of inner users across scenarios within a similar range. Thus, the adaptive strategy effectively maintains fairness within the inner group but does not automatically eliminate the gap with the outer group. This indicates that proportional bandwidth allocation is quite effective in preserving fairness in capacity among inner users, so that a significant gap is more visible between inner and outer users than between inner users. Further analysis indicates a consistent performance gap between inner and outer users in all scenarios. This gap persists due to a combination of two factors: low outer spectral efficiency due to poor channel conditions, and adaptive bandwidth sharing, which, although proportional, cannot compensate for the SINR loss in the outer group. This is influenced by several primary factors, i.e., the outer user's greater distance from the base station, greater path loss, exposure to heavier intercell interference, and the need to share bandwidth with a larger user population in the outer-dominant scenario.

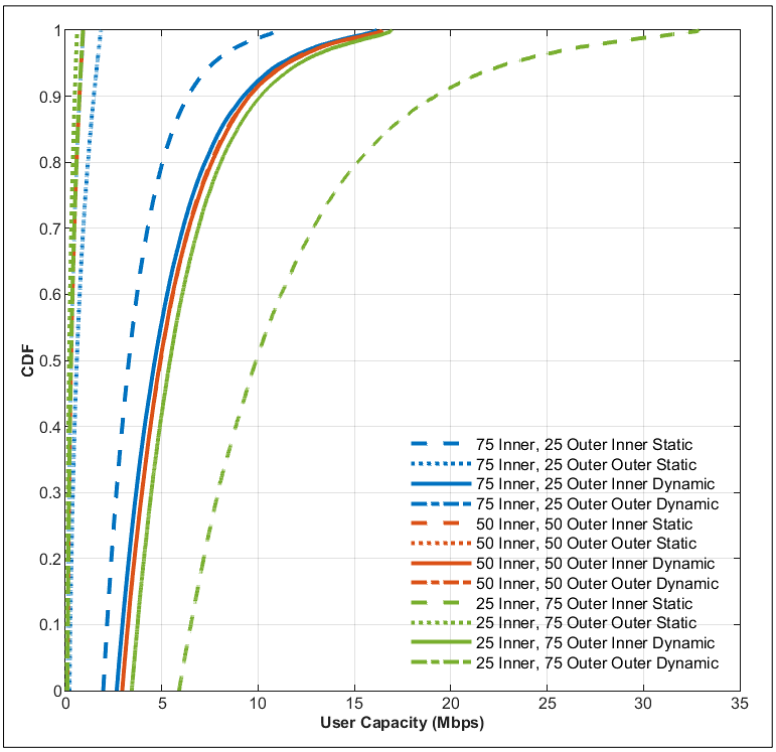

Figure 13. Comparison of user capacity for various user distributions under static and dynamic allocation

Figure 13 shows the user capacity CDF for the inner and outer layers under three user-proportion scenarios and two bandwidth allocation methods: static and dynamic. The graph shows that inner users consistently obtain significantly higher capacity than outer users, both under static and dynamic bandwidth allocation. Hence, the capacity gap between the two groups remains large in all scenarios. When looking at the CDF point of 0.9, which indicates that 90% of users have a capacity below that value, the difference between the groups is also striking. The horizontal distance between the curves at P90 can be interpreted as a "reliability gap" that directly relates to service experience; the wider the distance, the greater the potential for quality-of-service inequality. For example, in the static bandwidth scenario with 25 inner users and 75 outer users, 90% of inner users have a capacity below about 19 Mbps. In contrast, 90% of outer users have a capacity below about 0.3 Mbps. This comparison confirms that the static strategy in the outer-dominant scenario severely limits cell-edge users, even though the total bandwidth is the same. In the dynamic bandwidth scenario, the inner user capacity at the CDF 0.9 point tends to be more even, ranging from 8 to 10 Mbps across all scenarios. In contrast, the outer user capacity remains below 0.4 Mbps across all scenarios. This means that busy allocation effectively "uniforms" the performance of the inner group across scenarios. Still, for the outer group, the effect is small because the main bottleneck is channel-based (high path loss and intercell interference), resulting in disproportionate conversion of additional Hz into bits. This indicates that, while dynamic bandwidth is effective in balancing capacity between scenarios for inner users, improvements for outer users remain very limited, and the gap with inner users remains significant at high service probability levels.

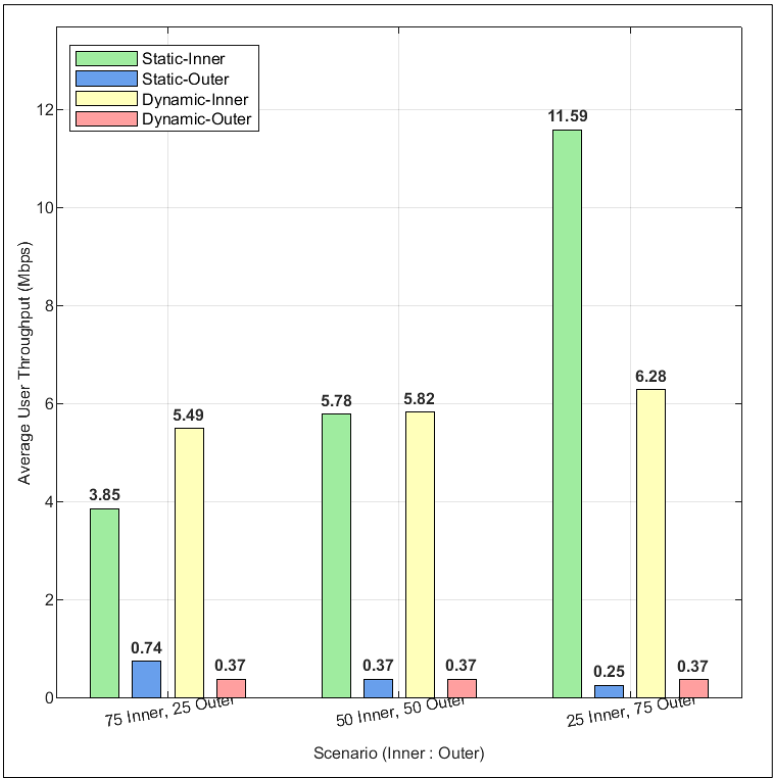

Figure 14. Average user capacity under static and dynamic allocation bandwidth for various user distributions

The bar chart in Figure 14 also confirms this phenomenon: dynamic bandwidth produces nearly equal average inner-user capacity across all three scenarios, whereas in the static bandwidth scenario, there is a significant disparity. This occurs because dynamic allocation allocates bandwidth portions proportionally to the number of users per layer, thereby reducing the "demand vs. supply" imbalance in the inner layer. In contrast, static allocation maintains a fixed share that can be inconsistent with user composition. For example, in the static bandwidth scenario with 25 inner and 75 outer users, the average inner-user capacity is 11.59 Mbps, while the average outer-user capacity is only 0.25 Mbps. The high inner value arises because a few inner users share a fixed portion of bandwidth. In contrast, the very low outer value reflects two overlapping factors: many users competing for that fixed portion and low spectral efficiency at the cell edge. In the 50:50 balance scenario, the average static inner-user capacity is 5.78 Mbps, while the average static outer-user capacity is only 0.37 Mbps. In a balanced composition, static allocation is indeed close to optimal in terms of proportion. However, the difference in inner–outer channel quality still keeps outer capacity in the low range.

This large gap is also seen in the 75:25 scenario, where inner users receive 3.86 Mbps and outer users 0.74 Mbps with static allocation. Although there are fewer outer users in the 75:25 configuration, the increased per-user quota cannot offset the SINR loss. However, with dynamic bandwidth allocation, inner user capacity becomes much more uniform across scenarios, with average values ranging from 5.49 to 6.28 Mbps (5.49 Mbps for the 75:25 scenario, 5.82 Mbps for the 50:50 scenario, and 6.28 Mbps for the 25:75 scenario), although outer user capacity remains low at around 0.37 Mbps across all scenarios. The narrow range indicates that adaptive mechanisms "normalize" inner performance across scenarios: when inner users are in the minority, the system increases the portion, and when inner users are in the majority, the portion is reduced to avoid waste, resulting in convergence. On the other hand, an almost constant outer capacity indicates a channel bottleneck; the additional Hz is not directly proportional to the bit at low SINR. Thus, although dynamic bandwidth allocation can improve the uniformity of inner user capacity across scenarios and improve the fairness of inner user distribution, the overall capacity gap between inner and outer users is still huge due to differences in physical conditions and interference, so the dynamic bandwidth allocation solution is more effective in reducing the inequality between scenarios for inner users but has not been fully able to overcome the disparity between the inner and outer layers, both on average and at high service probabilities such as at the CDF point of 0.9.

6- Conclusion

This paper introduces a unified numerical formulation for Fractional Frequency Reuse (FFR) and a user composition-based adaptive bandwidth allocation strategy specifically designed for multi-layer and multi-sector cellular networks. The proposed FFR metric explicitly accumulates sub-band usage at inner/outer layers (and inter-sectors), restoring classical 1/N reuse as a limit case while approaching full-reuse in coordinated multi-layer/sector operations. Thus, it provides a single, cross-architecture bridge from reuse to capacity.

Comprehensive simulations using a realistic urban macrocell model demonstrate that increasing the architectural complexity from a single-layer to a 2-layer 6-sector configuration can boost average cell capacity up to 184%. The results also reveal that dynamic bandwidth allocation, especially in scenarios dominated by inner users (75 inner, 25 outer), achieves the highest cell capacity, which is 41% higher than that of static bandwidth allocation. In addition, dynamic allocation improves fairness in outer user-dominated scenarios, with Jain's fairness index increasing to 0.444. These results emphasize the important function of the proposed numerical formulation and adaptive bandwidth management in maximizing spectrum usage, increasing overall capacity, and improving fairness across users in various deployment environments. The simulation and analytical results also point out that the performance of any bandwidth allocation approach is heavily dependent on user distribution patterns. Dynamic resource allocation yields considerable gain in the case of unbalanced traffic, whereas static allocation could be adequate if user distributions are steady and predictable.

Overall, this research contributes theoretically and practically to understanding resource management in next-generation cellular networks and provides valuable guidance for operators and researchers designing and implementing 5G cellular systems and beyond under various user and traffic distribution conditions.

7- Declarations

7-1- Author Contributions

Conceptualization, M.Y., I., M.S.A., and K.A.; methodology, M.Y., I., M.S.A., and K.A.; software, M.Y., M.S.A., and K.A.; validation, I., M.S.A., and M.Y.; formal analysis, I. and M.S.A.; investigation, I. and M.S.A.; resources, M.Y., I., M.S.A., and K.A.; data curation, M.Y. and I.; writing—original draft preparation, M.Y.; writing—review and editing, I., M.S.A., and K.A.; visualization, M.Y. and I.; supervision, I., M.S.A., and K.A.; project administration, I.; funding acquisition, M.Y. and M.S.A. All authors have read and agreed to the published version of the manuscript.

7-2- Data Availability Statement

The data presented in this study are available on request from the corresponding author.

7-3- Funding

This research is funded by Hibah PPMI ITB.

7-4- Institutional Review Board Statement

Not applicable.

7-5- Informed Consent Statement

Not applicable.

7-6- Conflicts of Interest

The authors declare that there is no conflict of interest regarding the publication of this manuscript. In addition, the ethical issues, including plagiarism, informed consent, misconduct, data fabrication and/or falsification, double publication and/or submission, and redundancies have been completely observed by the authors.

8- References

[1] Liu, G., Ding, X., Li, P., Zhang, L., Hu, C., & Xie, W. (2023). Novel Radio Resource Allocation Scheme in 5G and Future Sharing Network via Multi-Dimensional Collaboration. Electronics (Switzerland), 12(20), 4209. doi:10.3390/electronics12204209.

[2] Alsaedi, W. K., Ahmadi, H., Khan, Z., & Grace, D. (2023). Spectrum Options and Allocations for 6G: A Regulatory and Standardization Review. IEEE Open Journal of the Communications Society, 4, 1787–1812. doi:10.1109/OJCOMS.2023.3301630.

[3] Wang, D., Qiu, A., Zhou, Q., Partani, S., & Schotten, H. D. (2023). Investigating the Impact of Variables on Handover Performance in 5G Ultra-Dense Networks. Joint European Conference on Networks and Communications and 6G Summit, EuCNC/6G Summit 2023, 567–572. doi:10.1109/EuCNC/6GSummit58263.2023.10188324.

[4] Ahmad, I., & Hussain, A. (2023). Co-channel Interference Management for the Next-Generation Heterogeneous Networks using Deep Leaning. arXiv Preprint, arXiv:2301.10177. doi:10.48550/ARXIV.2301.10177.

[5] Seo, M., Chang, S. H., Lee, J. M., Kim, K. H., Park, H., & Kim, S. H. (2023). Optimal Coverage of Full Frequency Reuse in FFR Networks in Relation to Power Scaling of a Base Station. Sensors (Basel, Switzerland), 23(21), 8925. doi:10.3390/s23218925.

[6] Nasr-Esfahani, N., & Ghahfarokhi, B. S. (2021). Power management in green FFR-based heterogeneous cellular networks. Physical Communication, 46, 101285. doi:10.1016/j.phycom.2021.101285.

[7] Alzubaidi, O. T. H., Hindia, M. H. D. N., Dimyati, K., Noordin, K. A., Wahab, A. N. A., Qamar, F., & Hassan, R. (2022). Interference Challenges and Management in B5G Network Design: A Comprehensive Review. Electronics (Switzerland), 11(18), 2842. doi:10.3390/electronics11182842.

[8] Dong, H., Su, M., Liu, K., & Zou, W. (2020). Mitigation Strategy of Subsynchronous Oscillation Based on Fractional-Order Sliding Mode Control for VSC-MTDC Systems with DFIG-Based Wind Farm Access. IEEE Access, 8, 209242–209250. doi:10.1109/ACCESS.2020.3038665.

[9] Hanly, S. V., Liu, C., & Whiting, P. (2015). Capacity and stable scheduling in heterogeneous wireless networks. IEEE Journal on Selected Areas in Communications, 33(6), 1266–1279. doi:10.1109/JSAC.2015.2416971.

[10] Ge, X., Tu, S., Mao, G., Wang, C. X., & Han, T. (2016). 5G Ultra-Dense Cellular Networks. IEEE Wireless Communications, 23(1), 72–79. doi:10.1109/MWC.2016.7422408.

[11] Lam, S. C., & Tran, X. N. (2021). Fractional Frequency Reuse in Ultra Dense Networks. Physical Communication, 48, 101433. doi:10.1016/j.phycom.2021.101433.

[12] Yağcıoğlu, M. (2022). Dynamic resource allocation and interference coordination for millimeter wave communications in dense urban environment. Transactions on Emerging Telecommunications Technologies, 33(5), 4442. doi:10.1002/ett.4442.

[13] Chinipardaz, M., Amraee, S., & Sarlak, A. (2024). Joint downlink user association and interference avoidance with a load balancing approach in backhaul-constrained HetNets. PLoS ONE, 19(3 March), 298352. doi:10.1371/journal.pone.0298352.

[14] Alam, M. J., Chugh, R., Azad, S., & Hossain, M. R. (2024). Optimizing cell association in 5G and beyond networks: a modified load-aware biased technique. Telecommunication Systems, 87(3), 731–742. doi:10.1007/s11235-024-01202-w.

[15] Mughees, A., Tahir, M., Sheikh, M. A., Amphawan, A., Meng, Y. K., Ahad, A., & Chamran, K. (2023). Energy-efficient joint resource allocation in 5G HetNet using Multi-Agent Parameterized Deep Reinforcement learning. Physical Communication, 61, 102206. doi:10.1016/j.phycom.2023.102206.

[16] Khan, S. A., Kavak, A., Kucuk, K., & Asshad, M. (2019). A new fractional frequency reuse method for interference management in LTE-A HetNets. 27th Signal Processing and Communications Applications Conference, SIU 2019, 1–4. doi:10.1109/SIU.2019.8806317.

[17] Yin, Z. (2024). Coverage and capacity based inter-frequency handover in multi-layer networks. Heliyon, 10(4), 26225. doi:10.1016/j.heliyon.2024.e26225.

[18] Xie, Z., & Walke, B. (2010). Resource allocation and reuse for inter-cell interference mitigation in OFDMA based communication networks. The 5th Annual ICST Wireless Internet Conference, WICON 2010, 8489. doi:10.4108/ICST.WICON2010.8489.

[19] Bartsiokas, I. A., Gkonis, P. K., Kaklamani, D. I., & Venieris, I. S. (2022). ML-Based Radio Resource Management in 5G and Beyond Networks: A Survey. IEEE Access, 10, 83507–83528. doi:10.1109/ACCESS.2022.3196657.

[20] Trabelsi, N., Chaari Fourati, L., & Chen, C. S. (2024). Interference management in 5G and beyond networks: A comprehensive survey. Computer Networks, 239, 110159. doi:10.1016/j.comnet.2023.110159.

[21] Patil, A., Iyer, S., López, O. L. A., Pandya, R. J., Pai, K., Kalla, A., & Kallimani, R. (2024). A comprehensive survey on spectrum sharing techniques for 5G/B5G intelligent wireless networks: Opportunities, challenges and future research directions. Computer Networks, 253, 110697. doi:10.1016/j.comnet.2024.110697.

[22] Zhang, C., Lv, T., Huang, P., Lin, Z., Zeng, J., & Ren, Y. (2023). Joint Optimization of Bandwidth and Power Allocation in Uplink Systems with Deep Reinforcement Learning. Sensors, 23(15), 6822. doi:10.3390/s23156822.

[23] Wang, F., Chen, W., Tang, H., & Wu, Q. (2017). Joint optimization of user association, subchannel allocation, and power allocation in multi-cell multi-association OFDMA heterogeneous networks. IEEE Transactions on Communications, 65(6), 2672-2684. doi:10.1109/TCOMM.2017.2678986.

[24] Maaz, B., Khawam, K., Tohme, S., Lahoud, S., & Nasreddine, J. (2017). Joint user association, power control and scheduling in multi-cell 5G networks. IEEE Wireless Communications and Networking Conference, WCNC, 1–6. doi:10.1109/WCNC.2017.7925934.

[25] Wang, Y., Kumar, S., Garcia, L., Pedersen, K. I., Kovács, I. Z., Frattasi, S., Marchetti, N., & Mogensen, P. E. (2009). Fixed frequency reuse for LTE-advanced systems in local area scenarios. IEEE Vehicular Technology Conference, 1–5. doi:10.1109/VETECS.2009.5073560.